β-galactosidase-instructed intracellular nanofiber formation enhances tumor micro-PET imaging

Meimei Wang,[a] Kangxia Yu,[a] Dandan Zhu,[a] Pei Zou,[b] Peiyao Chen,[c] Hongyong Wang,[b] Yaling Liu,*[b] and Minhao Xie*[ab]

a School of Pharmacy, Nanjing Medical University, Nanjing 211166, China.

b NHC Key Laboratory of Nuclear Medicine, Jiangsu Key Laboratory of Molecular Nuclear Medicine, Jiangsu Institute of Nuclear Medicine, Wuxi 214063, China.

c Key Laboratory of Fermentation Engineering (Ministry of Education), National "111" Center for Cellular Regulation and Molecular Pharmaceutics, Hubei Key Laboratory of Industrial Microbiology, School of Food and Biological Engineering, Hubei University of Technology, Wuhan 430068, China.

E-mail: liuyaling@jsinm.org, xieminhao@jsinm.org

Experimental Supplementary Information

Materials and general methods

Chemical and materials: 2-(1*H*-benzotriazol-1-yl)-1,1,3,3-tetramethyluronium hexafluorophosphate (HBTU) and all the solid amino acids materials were purchased from GL Biochem(Shanghai)Ltd (Shanghai, China). 1-Hydroxybenzotriazole (HOBT) was purchased from Baomanbio (Shanghai, China). 2-(Naphthalen-2-yl)acetic acid was obtained from MACKLIN (Shanghai, China) and 2,3,4,6-Tetra-O-acetyl-α-D-galactopyranosyl bromide was obtained from Energy Chemical (Shanghai, China). β-Galactosidase (40 units/mg solid) for commercial use and solvents listed in this article

were obtained from J&K Scientific (Beijing, China). All the solid materials and solvents mentioned were used without additional purification. The Cell Counting Kit-8 was bought from Beyotime Biotechnology (Shanghai, China).

Instruments: ^{68}Ga was eluting from a ^{68}Ge/^{68}Ga generator (740 MBq, ITG Isotope Technologies Garching GmbH, Germany). Radio-HPLC analysis was performed on a Waters chromatography equipped with Waters 2998 Dual λ absorbance detector, the radio-detector (ElySia Raytest, Straubenhardt, Germany) and 1525 Binary HPLC Pump using an Inertsil ODS-3 column (5 μm, 4.6 mm × 250 mm, GL Sciences Inc.), H_2O / CH_3CN (A/B) mixed with 0.1% of trifluoroacetic acid (TFA) was used as the analysis and purification eluent. The spectra of high-resolution matrix-assisted laser desorption ionization time of flight mass spectrometry (HR-MALDI-TOF-MS) were recorded on an Ultraflextreme (Bruker Daltonics) and the electrospray ionization-mass spectrometry (ESI-MS) spectra were recorded via a quadrupole tandem mass equipped with SQ-detect 2 (Waters, USA). Transmission electron microscopy (TEM) images were obtained with a transmission electron microscope (JEOL JEM-2100) operating at an acceleration voltage of 200 kV. Micro-positron emission tomography (Micro-PET) imaging was operated on an Inveon scanner (Siemens, Germany). A γ-counter (2470, Perkin-Elmer Corporation, Waltham, MA, USA) was applied for radioactivity detection.

Enzyme kinetics: Different concentrations of Nap-1 were analyzed by HPLC to plot HPLC peak area *vs* Nap-1 amounts and obtain linear equation. β-gal (0.05 U μL^{-1}) with different concentrations of Nap-1G was incubated at 37°C for 5 min, then plotted initial velocities of β-gal enzyme-catalyzed reaction against the concentrations of Nap-1G and fitted to the Michaelis-Menten model.

Cell culture: OVCAR-3 cells were purchased from the BeNa Culture Collection (Henan, China) and routinely cultured in 80% Roswell Park Memorial Institute-1640 (RPMI-1640; Hyclone) supplemented with 20% fetal bovine serum and 0.01 mg/mL human insulin at 37℃ in a 5% CO_2 atmosphere.

Cell Counting Kit-8 test: Cell Counting Kit-8 (CCK-8) was used to evaluate the cytotoxicity of the compounds on OVCAR-3 ovarian cancer cells. 4×10^3 cells per well were seeded in a 96-well cell culture plate, and the cells were in the log phase. The cells were incubated for a whole night at 37°C with 5% CO_2. After removing the culture media from each well, the solutions of Nap-1G or Nap-1 (200 μL/well) were introduced at concentrations of 0, 50, 100 or 500 μM in the culture medium, respectively. The cells were cultured at 37°C for 12 or 24 h. Then, each well was added with CCK-8. After 2 h incubation, an enzyme-linked immunosorbent assay (ELISA) reader (BioTek uQuant, Winooski, VT, USA) was used to detect the absorption of the solution in each well at 450 nm. The viability of cell growth was calculated using the following formula: viability (%) = (mean of absorbance value of treatment group/mean of absorbance value of blank control) × 100.

Animal tumor model: Five-week-old female BALB/c nude mice were purchased from Changzhou Cavens Lab Animal Co. Ltd. (China) and used for animal experiments. All animals received care in compliance with the guidelines outlined in the Guide for the Care and Use of Laboratory Animals. The procedures were approved by the Animal Ethics Committee of Jiangsu Institute of Nuclear Medicine (IACUC number: JSINM-2021-038 and JSINM-2022-027). Each mouse received a subcutaneous administered injection of 5×10^6 OVCAR-3 cancer cells into the armpit. The mice were then used in successive studies up until the tumor sizes reached 5 mm in diameter.

In vivo micro-PET imaging: Two groups of OVCAR-3 tumor-bearing mice (n = 4 per group) were randomly assigned. One group was injected with 1.2-3.8 MBq of [^{68}Ga]Nap-1G intravenously; the other was injected with [^{68}Ga]Nap-1. Ten-minute static PET images were obtained at 30, 60, 90 and 120 min post-injection. The whole-body coronal image reconstruction was conducted by 3D OSEM. Vendor software (ASIPro VM 6.8.6.9) was applied to draw regions of interest (ROIs) in the tumor and liver according to each micro-PET scan. The mean PET units of three consecutive slices were averaged to obtain the mean radioactivity concentration. By using a conversion factor and the administered activity, the % ID/g mean was calculated.

Ex vivo biodistribution: OVCAR-3 tumor-bearing mice were randomly divided into 2 groups (n=6 per group). 1.7-3.0 MBq [^{68}Ga]Nap-1G was injected into one group via the tail vein, and similar radioactivity of [^{68}Ga]Nap-1 was injected into the other group. At the selected time point (1 h and 2 h), the mice were sacrificed and the major organs (brain, heart, liver, spleen, lung, kidney, stomach, bone, muscle, intestines and tumor) were taken out to weigh. A γ-counter was employed to measure the radioactivity of each organ. By using a conversion factor and the administered activity, % ID/g was calculated.

Hematoxylin-eosin (HE) staining: Nude mice injected with saline were the control group, and the experimental group was injected with [^{68}Ga]Nap-1G. Major organs including (brain, heart, liver, spleen, lung, and kidney) were taken out 2 h post-injection. Each organ was put in tissue processor to dehydrate at 4°C overnight. Afterward, organs were frozen and sliced into a section thickness of 6 μm. and all slices were placed in a 37°C drying oven overnight. Then HE staining kit was applied to stain the tissue sections. Finally, images were obtained via a fluorescence microscope.

Synthesis and characterization of Y(GalAc)-OtBu (B)

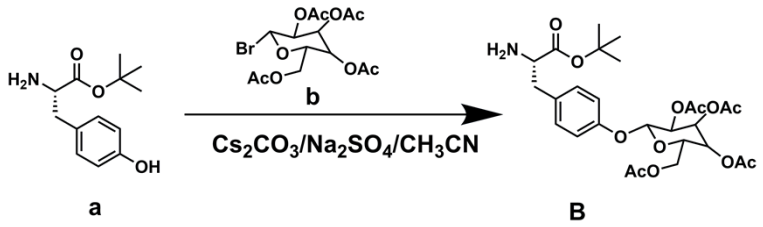

Scheme S1. Synthesis route for compound B.

Tyr-tBu (a, 118.57 mg, 0.5 mmol), Na_2SO_4 (177.55 mg, 1.25 mmol) and Cs_2CO_3 (814.55 mg, 2.5 mmol) were dissolved in CH_3CN. Further magnetic stirring was carried out at room temperature under N_2 for 16 h after adding 2,3,4,6-Tetra-O-acetyl-α-D-galactopyranosyl bromide (b, 205.01 mg, 0.5 mmol) to the mixture. The pure product was obtained after HPLC purification (yield: 119.23 mg, 0.21 mmol, 42%). MS: calculated for $C_{27}H_{37}NO_{12}$ $[M + H]^+ = 568.23$, obsvd. ESI-MS: m/z 568.50.

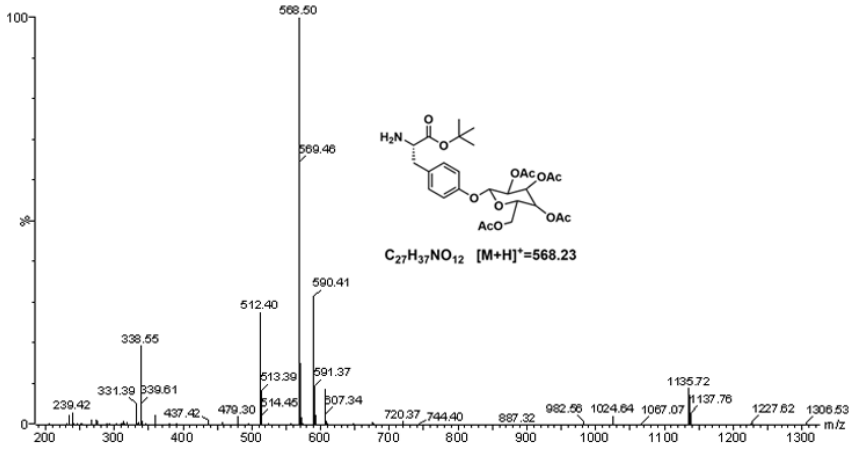

Fig. S1. ESI-MS spectrum of compound B.

Preparations of Nap-FFFK(DOTA-^{68}Ga)Y(Gal)-OH ([^{68}Ga]Nap-1G)

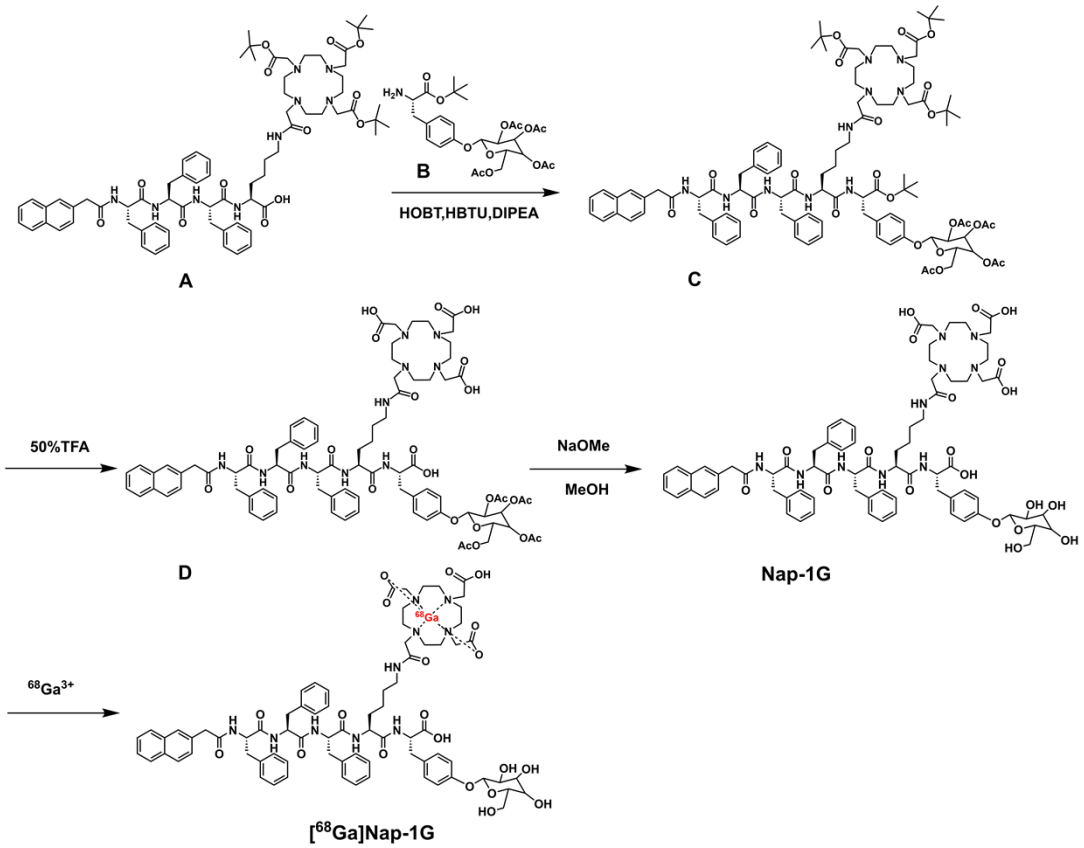

Scheme S2. Synthesis route for compounds A, C, D, Nap-1G and [^{68}Ga]Nap-1G.

The synthesis route for compounds A, C, D, Nap-1G and [^{68}Ga]Nap-1G were shown in Scheme S2.

Synthesis and characterization of Nap-FFFK(DOTA(tBu)$_3$)-OH (A): Nap-FFFK(DOTA(tBu)$_3$)-OH (A) was synthesized by standard solid-phase peptide synthesis (yeild: ~90%). MS: calculated for $C_{73}H_{99}N_9O_{13}$ $[M + H]^+$ = 1310.74, obsvd. ESI-MS: m/z 1310.98.

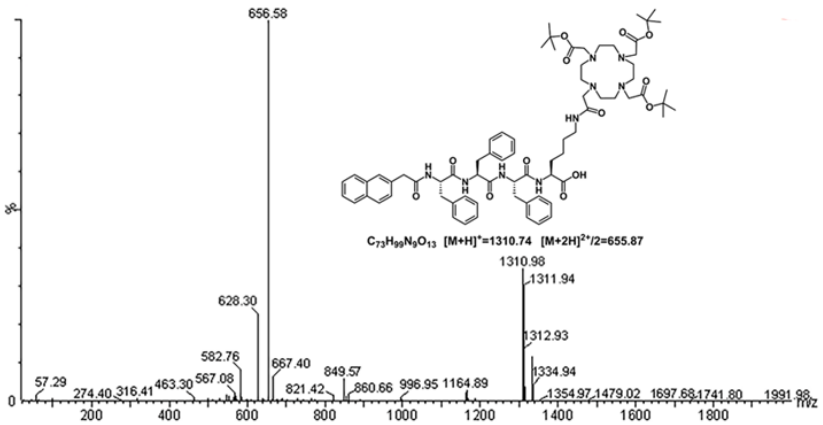

Fig. S2. ESI-MS spectrum of compound A.

Synthesis and characterization of Nap-FFFK(DOTA)Y(GalAc)-OH (D): Compound A (0.01 mmol, 13 mg), compound B (0.01 mmol, 5.7 mg), 1-Hydroxybenzotriazole (HOBT, 0.01 mmol, 1.4 mg), and 2-(1*H*-benzotriazol-1-yl)-1,1,3,3-tetramethyluronium hexafluorophosphate (HBTU, 0.01 mmol, 3.8 mg) in 5 mL N, N'-dimethyl formamide (DMF) were stirred 4 h at room temperature after adding N, N-diisopropylethylamine (DIPEA, 0.01 mmol, 2 μL) under nitrogen atmosphere. The pure product of compound C was obtained after HPLC purification(yield: 10.1 mg, 0.005 mmol, 54%). The tBu protecting groups of compound C were cleaved with dichloromethane (DCM, 5 mL) and Triisopropylsilane (TIPS, 200 μL) in trifluoroacetic acid (TFA, 5 mL) for 3 h at 0°C. The cleavage agent was then again added after the mixture had been condensed using a rotary evaporator. Three times were repeated, and the reaction was completed. The pure product was obtained after HPLC purification (yield: 4.6 mg, 0.003 mmol, 56%), MS: calculated for $C_{84}H_{102}N_{10}O_{24}$ $[M + 2H]^{2+}/2$ = 818.36, obsvd. ESI-MS: m/z 819.06.

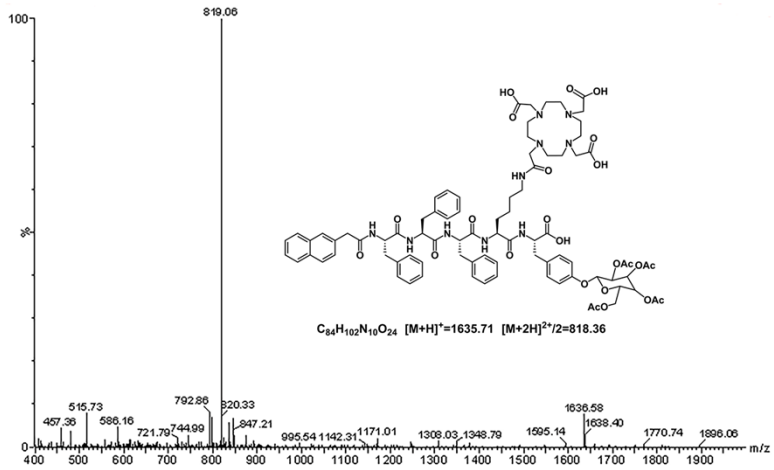

Fig. S3. ESI-MS spectrum of compound D.

Synthesis and characterization of Nap-FFFK(DOTA)Y(Gal)-OH (Nap-1G): Compound D (8 mg, 0.005 mmol) and Sodium methoxide (NaOMe,16.9 mg, 0.3 mmol)

were dissolved in methanol (MeOH), then stirred magnetically at room temperature for three hours. After adding HCl to acidify the mixture to around pH 4, HPLC was employed for the purification (yield: 4.1 mg, 0.003 mmol, 56%). MS: calculated for $C_{76}H_{94}N_{10}O_{20}$ $[M+H]^+$ = 1467.6646, obsvd. HR-MALDI-MS: m/z 1467.5552.

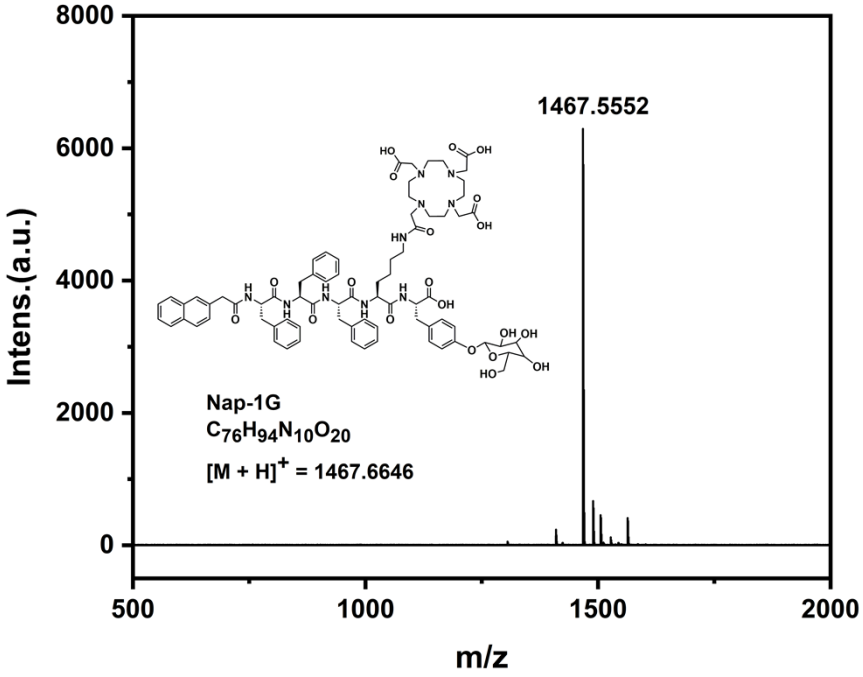

Fig. S4. HR-MALDI-MS spectrum of Nap-1G.

Synthesis of Nap-FFFK(DOTA-^{68}Ga)Y(Gal)-OH ([^{68}Ga]Nap-1G): The $^{68}Ga^{3+}$ activity was eluted from the ^{68}Ge/^{68}Ga generator with 0.05 M ultrapure HCl. To 800 μL main fraction of the generator elution (~100 MBq), 200 μL 0.25 M sodium acetate solution was added and the pH value was adjusted to 4-5, then 10 μL of Nap-1G dissolved in water (1 mM) was added. The mixture was heated at 95°C for 10 min, detected with a radio-HPLC system (retention time 11.4 min), and the radiochemical purity was above 97%.

Preparations of Nap-FFFK(DOTA-^{68}Ga)Y-OH ([^{68}Ga]Nap-1)

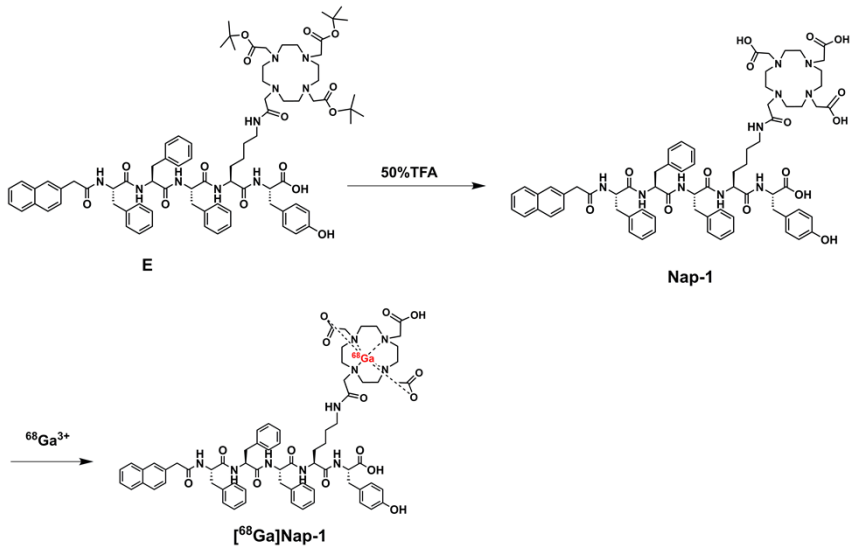

Scheme S3. Synthesis route of compound Nap-1 and [^{68}Ga]Nap-1.

Synthesis and characterization of Nap-FFFK(DOTA(tBu)$_3$)Y-OH (E): Nap-FFFK(DOTA(tBu)$_{3)}$Y-OH (E) was synthesized through solid-phase peptide synthesis (yield: ~ 90%). MS: calculated for $C_{82}H_{108}N_{10}O_{15}$ $[M+2H]^{2+}/2$ = 737.40, obsvd. ESI-MS: m/z 738.22.

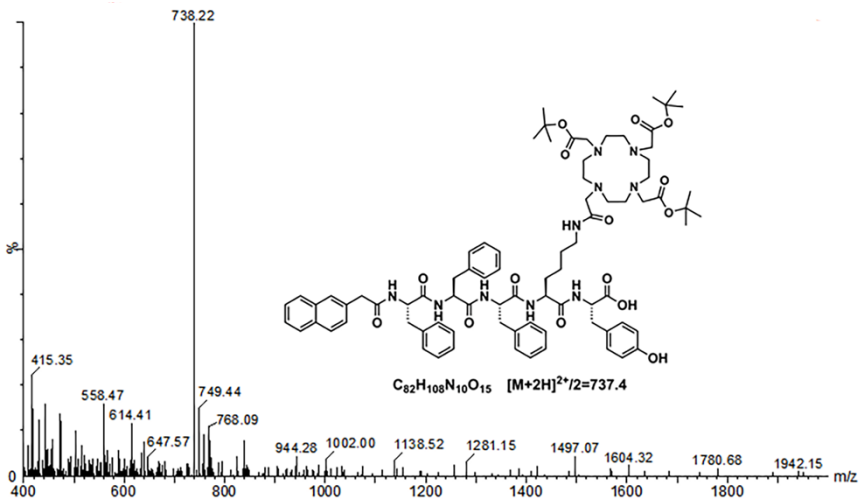

Fig. S5. ESI-MS spectrum of compound E.

Synthesis of Nap-FFFK(DOTA)Y-OH (Nap-1): The tBu protecting groups of compound E were cleaved with DCM (5 mL) and TIPS (200 μL) in TFA (5 mL) for 3 h at 0ºC; then the mixture was concentrated by a rotary evaporator before adding the previous cleavage reagent. The reaction was completed after being repeated three times. The pure product of Nap-1 was obtained after HPLC purification (yield: ~ 60%). MS: calculated for $C_{70}H_{84}N_{10}O_{15}$ $[M+H]^+$ = 1305.4970, obsvd. HR-MALDI-MS: m/z

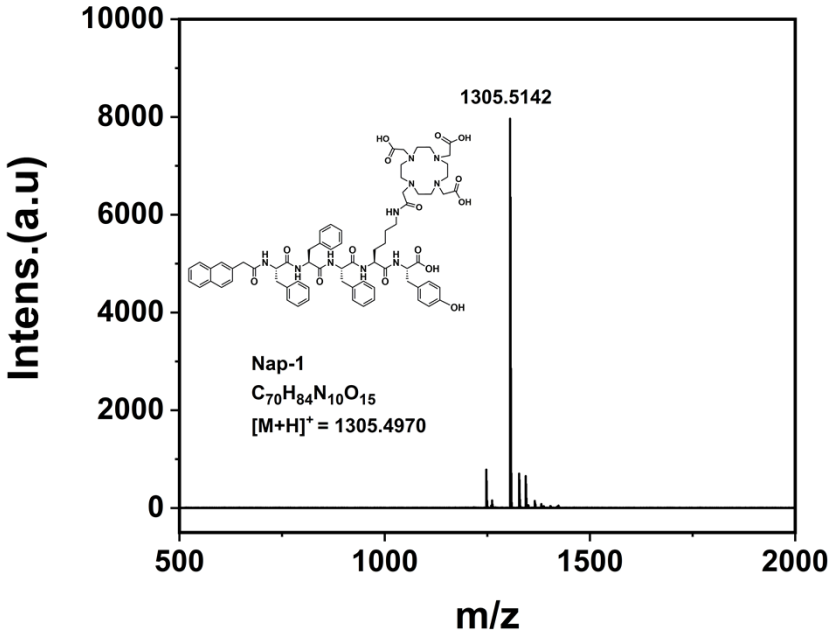

1305.5142.

Fig. S6. HR-MALDI-MS spectrum of Nap-1.

Synthesis of Nap-FFFK(DOTA-^{68}Ga)Y-OH ([^{68}Ga]Nap-1): The $^{68}Ga^{3+}$ activity was eluted from the ^{68}Ge/^{68}Ga generator with 0.05 M ultrapure HCl. To 800μL main fraction of the generator elution (~ 100 MBq), 200 μL 0.25 M sodium acetate solution was added, and the pH value was adjusted to 4-5, then 10 μL of Nap-1 dissolved in water (1 mM) was added. The mixture was heated at 95ºC for 10 min, the reaction was detected with a radio-HPLC system (retention time 13.7 min), and the radiochemical purity was above 97%.

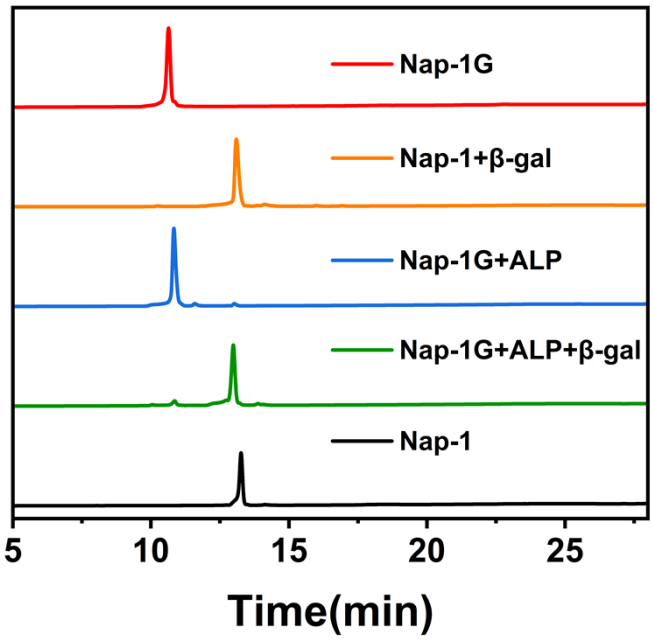

Fig. S7. HPLC traces of Nap-1G (red), 500 μM Nap-1 incubated with β-gal (0.08 U μL^{-1}) at 37°C for 10 min (orange), 500 μM Nap-1G incubated with ALP (0.08 U μL^{-1}) at 37°C for 10 min (blue), 500 μM Nap-1G incubated with β-gal (0.08 U μL^{-1}) and ALP (0.08 U μL^{-1}) at 37°C for 10 min (green), Nap-1 (black).

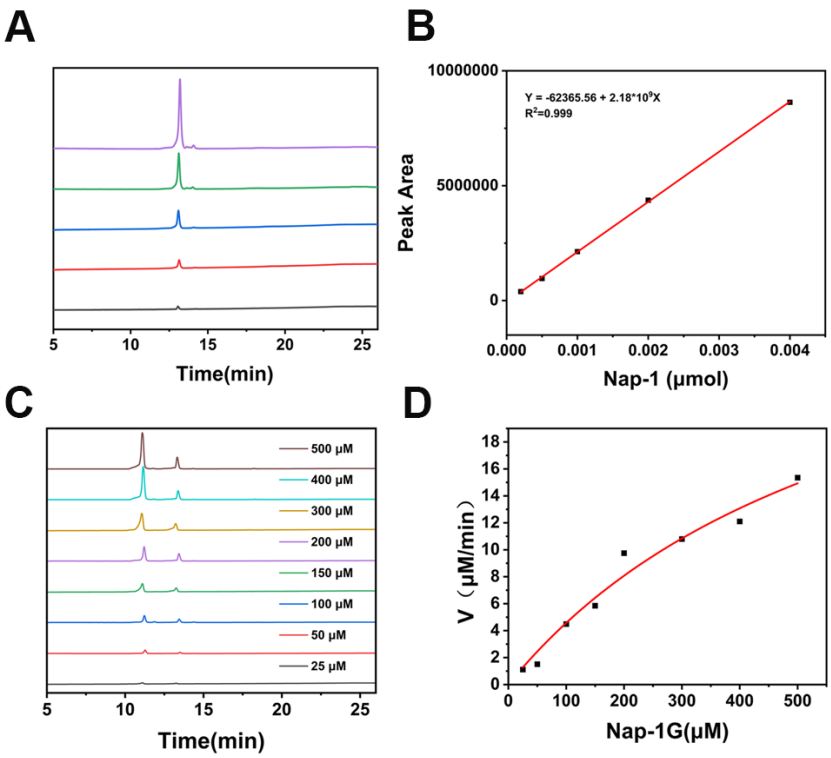

Fig. S8. (A) HPLC traces of different concentrations of Nap-1. (B) Plotting of the HPLC peak areas *vs.* the Nap-1 amounts. (C) HPLC traces of different concentrations of Nap-1G incubated with β-gal (0.05 U μL^{-1}) at 37°C for 5 min. (D) Michaelis-Menten plot of the β-gal enzyme-catalyzed reaction of Nap-1G.

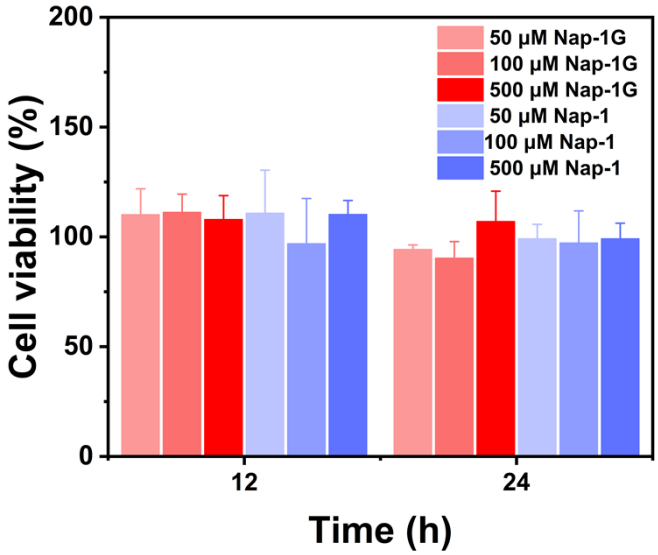

Fig. S9. Biocompatibility test of 50 µM, 100 µM or 500 µM of Nap-1G (red) or Nap-1 (blue) on OVCAR-3 cells. Results are presented as mean ± SD, n = 4 independent experiments.

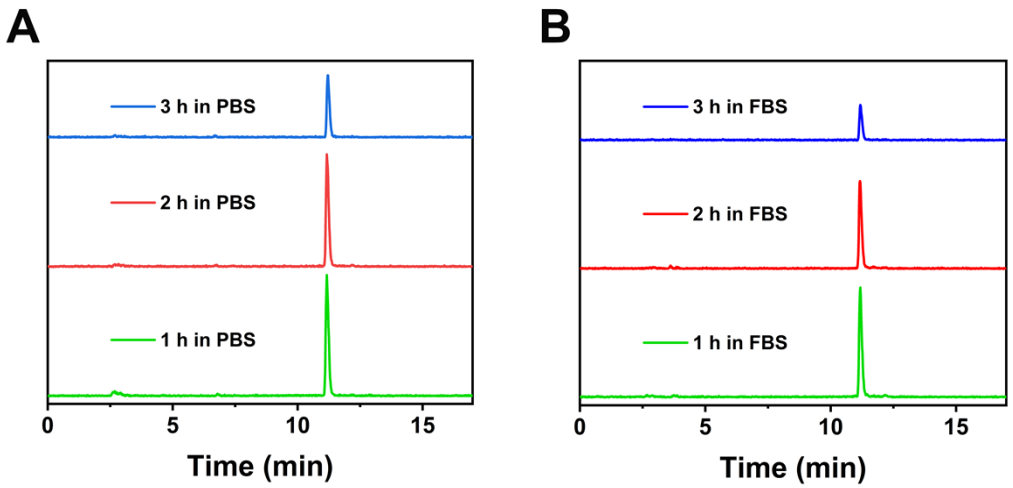

Fig. S10. Stability experiment of [^{68}Ga]Nap-1G in PBS (A) and FBS (B) after incubating 1, 2, 3 h, monitoring by a radio-HPLC.

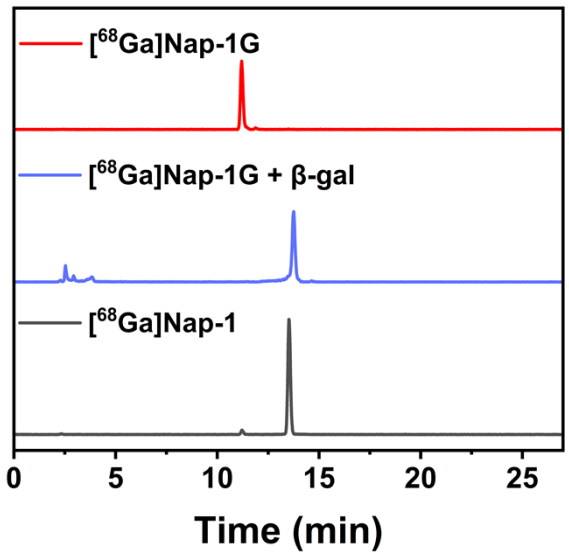

Fig. S11. Radioactive enzymatic hydrolysis of [^{68}Ga]Nap-1G.

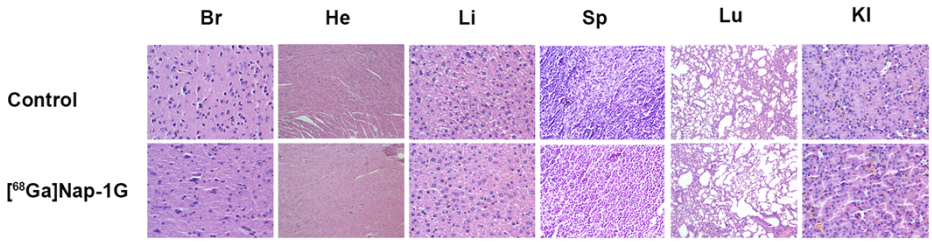

Fig. S12. HE staining of the major organs (brain (Br), heart (He), liver (Li), spleen (Sp), lung (Lu), kidney (Ki)) of the nude mice sacrificed at 2 h post-injection of saline (Control), 4.5 MBq [^{68}Ga]Nap-1G.

Supplementary tables

Table S1. HPLC conditions for analysis of all compounds.

Time (min)	Flow (mL/min)	H_2O % (0.1% TFA)	MeCN % (0.1% TFA)
0	1	70	30
1	1	70	30
20	1	30	70
25	1	30	70
30	1	70	30

Table S2. HPLC conditions for purification of compounds.

Time (min)	Flow (mL/min)	H_2O % (0.1% TFA)	MeCN % (0.1% TFA)
0	3	60	40
1	3	60	40
15	3	50	50
25	3	20	80
30	3	60	40